This is the accepted manuscript made available via CHORUS. The article has been published as:

Fourier coefficients of noninterdependent collective motions in heavy-ion collisions

Zhiwan Xu, Gang Wang, Aihong Tang, and Huan Zhong Huang

Phys. Rev. C **107**, L061902 — Published 23 June 2023

DOI: 10.1103/PhysRevC.107.L061902

Fourier Coefficients of Non-interdependent Collective Motions in Heavy-ion Collisions

Zhiwan Xu,[1,*] Gang Wang,[1,†] Aihong Tang,[2] and Huan Zhong Huang[1,3]

[1] *Department of Physics and Astronomy, University of California, Los Angeles, California 90095, USA*
[2] *Brookhaven National Laboratory, Upton, New York 11973*
[3] *Key Laboratory of Nuclear Physics and Ion-beam Application (MOE), and Institute of Modern Physics, Fudan University, Shanghai-200433, People's Republic of China*

We present a novel scenario in heavy-ion collisions where different modes of collective motions are non-interdependent, driven by factorized actions in the created nuclear medium. Such physics mechanisms could each dominate at a distinct evolution stage, or coexist simultaneously. If the probability of particle emission is modulated by each non-dependent collective motion with a single-harmonic Fourier expansion, the particle azimuthal distribution should be the product of all these expansions. Consequently, non-leading cross terms between collectivity modes appear, and their contributions to experimental observables could be significant. In particular, we argue that the chiral magnetic effect (CME) and elliptic flow can develop separately, with their convolution affecting the observable that is sensitive to the shear-induced CME. We will use the event-by-event anomalous-viscous fluid dynamics model to illustrate the effects of this scenario. Besides giving new insights into searches for the CME, we also propose feasible experimental tests based on conventional flow harmonics, and demonstrate the emergence of non-leading cross terms with a multi-phase transport model.

keywords: chiral magnetic effect; elliptic flow; heavy-ion collision; non-interdependent

In high-energy heavy-ion collisions, the emission pattern of final-state particles reveals different collectivity modes of the created nuclear medium. Figure 1 illustrates a few examples of collective motions at mid-rapidities in non-central collisions. A particular concept is the reaction plane, spanned by impact parameter (x-axis) and beam momenta (z-axis). (a) In the reaction plane, a slightly tilted participant region [1] violates the boost invariance, and leads to a rapidity-odd emission of produced particles, known as directed flow (v_1). (b) When viewed along the beam line, the almond-shaped overlap zone in coordinate space is transformed via a hydrodynamic expansion [2] into a rapidity-even degeneracy between in-plane and out-of-plane emissions, called elliptic flow (v_2). (c) The chiral magnetic effect (CME) [3] induces an out-of-plane electric charge separation ($a_1^{\pm}$), provided that a quark chirality imbalance emerges from the chiral anomaly [4], and an intense magnetic field ($\vec{B}$) is generated by protons from the colliding nuclei [5]. (d) Recently, a higher-order effect, the shear-induced CME (siCME) [6] has been proposed, in which the combination of magnetic field and hydrodynamic shear creates a charge-dependent triangular flow ($a_3^{\pm}$).

To quantify the collective motions in a given kinematic region, it is convenient to decompose the azimuthal angular (φ) distribution of produced particles in each collision with a Fourier series [7]:

$$\frac{2\pi}{N^{\pm}}\frac{dN^{\pm}}{d\varphi} = 1+\sum_{n=1}^{\infty} 2a_n^{\pm}\sin n\Delta\varphi+\sum_{n=1}^{\infty} 2v_n^{\pm}\cos n\Delta\varphi, \quad (1)$$

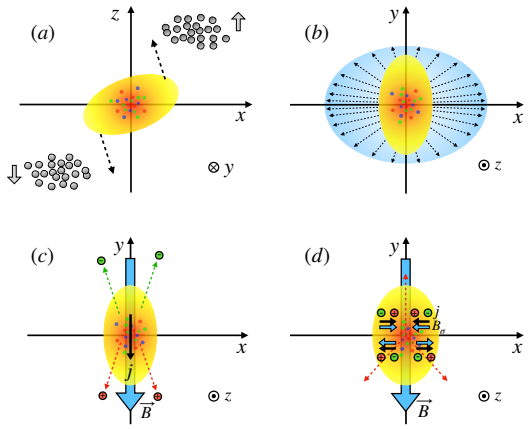


FIG. 1. Illustration of collective motions in heavy-ion collisions: (a) directed flow, (b) elliptic flow, (c) the CME-induced electric current j along the $\vec{B}$ field, and (d) the siCME-induced charge-dependent triangular emission. The dashed arrows represent produced-particle momenta. B_σ denotes the new component of the $\vec{B}$ field caused by its interplay with shear flow.

where $\Delta\varphi$ is the azimuthal angle of a particle relative to the reaction plane, and the superscripts $+$, $-$ indicate the charge signs. For simplicity, we will omit these superscripts in the following discussions, and express them only where necessary. The coefficients $a_n \equiv \langle \sin n\Delta\varphi\rangle$ and $v_n \equiv \langle \cos n\Delta\varphi\rangle$ are experimentally obtainable by averaging over particles of interest and over events. While Fourier-expanding a probability distribution is always a useful approach, establishing the relationship between the Fourier coefficients and underlying physics mechanisms can be nontrivial. Storing coefficients in an or-

* zhiwanxu@physics.ucla.edu
† gwang@physics.ucla.edu

thonormal basis implies that each collectivity mode is treated as a non-dependent action on the final-state particle distribution. However, this leads to a logical inconsistency. If the collectivity modes are orthogonal or non-interdependent, each action should modulate the probability of particle emission with its own single-harmonic ($\tilde{a}_n$ or $\tilde{v}_n$) Fourier expansion. According to the rule of multiplication for independent actions, it is the product, rather than the sum, of these short expansions that describes the particle azimuthal distribution. Then, the a_n (v_n) measured from a long linear Fourier expansion as in Eq. (1) may not be independent of each other, and may not fully match the true $\tilde{a}_n$ ($\tilde{v}_n$) of the pertinent physics process.

In general, factorized actions, such as distinct physics mechanisms, could occur concurrently, but do not rely on each other's existence during evolution. As long as the collective motions have separate evolution paths to affect particle emission, we consider them to be not coordinated with each other and approximate the particle distribution with the factorized form of Fourier expansions. For example, elliptic flow can be developed regardless of the presence of the CME, and vice versa. Then, $\tilde{a}_1$ and $\tilde{v}_2$ should appear in two separate Fourier expansions, $(1+2\tilde{a}_1 \sin\Delta\varphi)$ and $(1+2\tilde{v}_2 \cos 2\Delta\varphi)$, respectively, and their product specifies the final-state particle distribution. Compared with Eq. (1), the factorized form provides a non-leading cross term:

$$\begin{aligned} &4\tilde{a}_1\tilde{v}_2 \sin\Delta\varphi \cos 2\Delta\varphi \\ &= -2\tilde{a}_1\tilde{v}_2 \sin\Delta\varphi + 2\tilde{a}_1\tilde{v}_2 \sin 3\Delta\varphi. \end{aligned} \tag{2}$$

In this case, the a_1 and a_3 manifested in the linear Fourier expansion deviate from the true $\tilde{a}_1$ and $\tilde{a}_3$, respectively.

Under the hypothesis that the actions responsible for collective motions can be factorized, the particle azimuthal distribution would be expressed naturally as

$$\frac{2\pi}{N^\pm}\frac{dN^\pm}{d\varphi} = \prod_{n=1}^{\infty}(1+2\tilde{a}_n^\pm \sin n\Delta\varphi)\prod_{n=1}^{\infty}(1+2\tilde{v}_n^\pm \cos n\Delta\varphi). \tag{3}$$

Note that Eq. (3) is not a replacement of Eq. (1), but they are two representations of the same distribution with different emphases, and both are applicable to real-data analyses. The coefficients in the former expansion represent the strengths of the collective motions driven by factorized actions, whereas those in the latter denote the final emergent collectivity modes. Typically, flow and CME measurements are conducted using multi-particle correlations based on the definition in Eq. (1), and the results thus obtained manifest v_n (a_n), which can be readily demodulated into $\tilde{v}_n$ ($\tilde{a}_n$).

In reality, the difference between a_n and $\tilde{a}_n$ or between v_n and $\tilde{v}_n$ is negligible for many harmonics. For example, the magnitude of $\tilde{a}_n\tilde{a}_m$ could be much smaller than $\tilde{v}_{n+m}$ or $\tilde{v}_{|n-m|}$. We will focus on three coefficients: $\tilde{a}_1$, $\tilde{a}_3$ and $\tilde{v}_2$, and study how they are related to their counterparts, a_1, a_3 and v_2. Directed flow is not included, because v_1 is a rapidity-odd function in symmetric collisions, and its rapidity-integrated contribution to other coefficients will be zero in most cases. Now, Eq. (3) takes a specific form:

$$\begin{aligned} \frac{2\pi}{N^\pm}\frac{dN^\pm}{d\varphi} \propto (1+2\tilde{a}_1^\pm \sin\Delta\varphi) \times (1+2\tilde{a}_3^\pm \sin 3\Delta\varphi) \\ \times(1+2\tilde{v}_2^\pm \cos 2\Delta\varphi). \end{aligned} \tag{4}$$

By comparing Eqs. (1) and (4), we find the following connections between phenomena and noumena,

$$a_1 = \tilde{a}_1 - \tilde{a}_1\tilde{v}_2 + \tilde{a}_3\tilde{v}_2, \tag{5}$$

$$a_3 = \tilde{a}_3 + \tilde{a}_1\tilde{v}_2, \tag{6}$$

$$v_2 = \tilde{v}_2 + \tilde{a}_1\tilde{a}_3. \tag{7}$$

Here we ignore any higher-order term involving $\tilde{a}_1\tilde{a}_3\tilde{v}_2$.

Since the magnitude of $\tilde{a}_1\tilde{a}_3$ is typically lower than that of v_2 by a few orders of magnitude, v_2 and $\tilde{v}_2$ are almost the same. We will abandon $\tilde{v}_2$, and only use v_2 in the following discussions. Given that the siCME-induced $\tilde{a}_3$ is much smaller than the CME-induced $\tilde{a}_1$, Eq. (5) indicates that the observed a_1 roughly equals $\tilde{a}_1(1-v_2)$. Furthermore, Eq. (6) asserts that the observed a_3 contains a contribution of $\tilde{a}_1 v_2$ on top of the primordial $\tilde{a}_3$, if any. For completeness, we also express $\tilde{a}_1$ and $\tilde{a}_3$ in terms of experimental observables:

$$\tilde{a}_1 = \frac{a_1 - a_3 v_2}{1 - v_2 - v_2^2}, \tag{8}$$

$$\tilde{a}_3 = \frac{a_3 - a_1 v_2 - a_3 v_2}{1 - v_2 - v_2^2}. \tag{9}$$

We use the Event-by-Event Anomalous-Viscous Fluid Dynamics (EBE-AVFD) model [8–10] to test our inferences from factorized actions via relations derived in Eqs. (5) and (6). The EBE-AVFD event generator simulates the dynamical CME transport for u, d and s quarks in addition to the hydrodynamically expanding viscous medium in heavy-ion collisions, and properly handles local charge conservation and resonance decays. We have analyzed 5.8×10^7 events of Au+Au collisions at $\sqrt{s_{NN}} = 200$ GeV in the 30–40% centrality range, using the same settings and input parameters as adopted in Ref. [11]. For simplicity, we will use the true reaction plane to perform the simulation analysis, and ignore the possible fluctuation effects concerning the observables of elliptic flow and the CME.

The initial conditions for entropy density (s) profiles and for electromagnetic field vary in accordance with the event-by-event nucleon configuration from the Monte Carlo Glauber simulations [12]. The chirality charge density (n_5) is implemented in the form of n_5/s, which controls the strength of the CME transport. In this study, we take a modest value of $n_5/s = 0.1$, the same as used in Ref. [6].

The medium expansion is managed by the VISH2+1 simulation package [13], which is a boost-invariant hydrodynamics framework. Consequently, directed flow vanishes, and elliptic flow is a major collectivity mode. In these EBE-AVFD calculations, magnetic field is set to

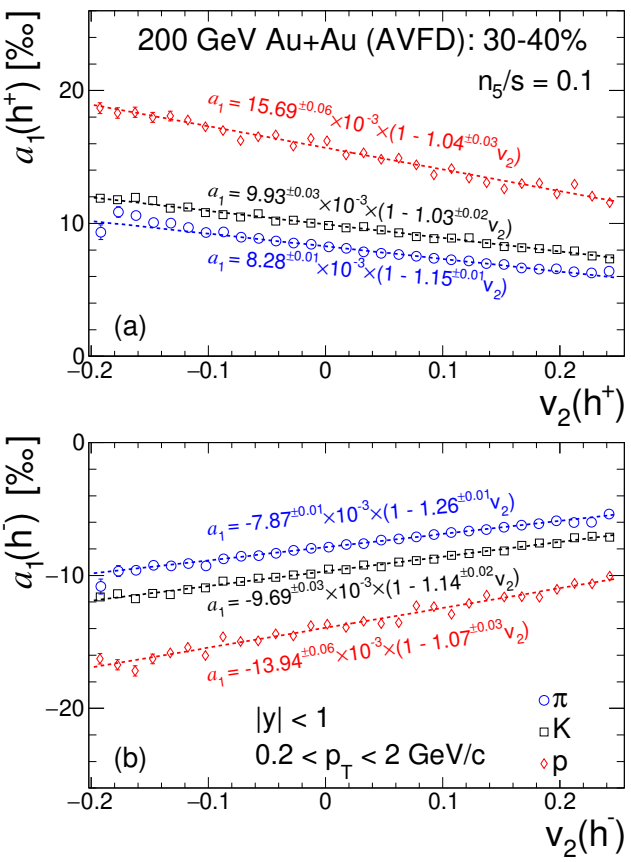


FIG. 2. Correlations between a_1 and v_2 calculated on an event-by-event basis from EBE-AVFD simulations of 30–40% Au+Au collisions at $\sqrt{s_{NN}} = 200$ GeV for (a) π^+, K^+ and p, and for (b) π^-, K^- and $\bar{p}$. The fit function, $a_1(v_2) = a_1(0) \times (1 + Cv_2)$, returns C close to -1 for all the cases.

last long enough, so that for a substantial time period the CME does coexist with the hydrodynamic formation of elliptic flow. However, the dynamical CME transport is governed by anomalous hydrodynamic equations as a linear perturbation on top of the medium flow background, since the back-reaction of finite chiral quark densities is negligible in collisions at $\sqrt{s_{NN}} = 200$ GeV [8]. Therefore, the two modes of collective motions featuring $\tilde{a}_1^{\pm}$ and v_2, respectively, develop independently of each other, and satisfy the generalized criterion for non-interdependent collective motions. We do not invoke the siCME in these simulations, and thus $\tilde{a}_3^{\pm}$ is zero. Accordingly, Eqs. (5) and (6) become as simple as

$$a_1 = \tilde{a}_1(1 - v_2), \tag{10}$$

$$a_3 = \tilde{a}_1 v_2. \tag{11}$$

Figure 2 shows the observed a_1 vs v_2 from EBE-AVFD simulations of Au+Au collisions at $\sqrt{s_{NN}} = 200$ GeV in the centrality interval of 30–40% for (a) π^+, K^+ and p, and for (b) π^-, K^- and $\bar{p}$. Both a_1 and v_2 are calculated on an event-by-event basis within the rapidity range of $|y| < 1$ and the transverse momentum range of $0.2 < p_T < 2$ GeV/c. For all the particle species, a linear correlation is present between a_1 and v_2. The fit function (dashed lines), $a_1(v_2) = a_1(0) \times (1 + Cv_2)$, renders the parameter C close to -1 for all the cases, seemingly supportive of Eq. (10). However, we cannot claim unambiguous evidence for the scenario of factorized actions based solely on this slope parameter, due to the trigonometric identity

$$\sin^2 \Delta\varphi \equiv (1 - \cos 2\Delta\varphi)/2. \tag{12}$$

Even when both a_1 and v_2 are averaged over particles in each event before being correlated, the correlation could still be dominated by the mathematical relation. In addition, there could be an anti-correlation between the $\tilde{a}_1$ magnitude itself and v_2, especially for pions. This higher-order effect may arise from resonance decays, since secondary particles will smear and dilute the $\tilde{a}_1$ value averaged over all pions [8], while inheriting a larger v_2 from resonances at higher p_T [14, 15]. The $a_1(0)$ or $\tilde{a}_1$ values retrieved from the fits also exhibit a particle-species dependence, which could be partially explained by the mean p_T effect. Similar to v_2, the $\tilde{a}_1$ magnitude increases with p_T at the low-p_T region [8], and pions, kaons, and protons form an ascending order of mean p_T. The quark coalescence mechanism [16] could also play a role by making the $\tilde{a}_1$ magnitude larger for baryons than for mesons at the intermediate-p_T region.

Figure 3 shows EBE-AVFD calculations of the observed a_3 as a function of p_T in 30–40% Au+Au collisions at 200 GeV for (a) π^+ and π^-, for (b) K^+ and K^-, and for (c) p and $\bar{p}$. Although the a_3 magnitudes for pions and protons are comparable to the corresponding predictions for the siCME-induced a_3 (as shown in the upper panel of Fig. 3 in Ref. [6]), our simulations do not entail the siCME. On the contrary, we depict $a_1 v_2/(1 - v_2)$ or $\tilde{a}_1 v_2$ with shaded bands, which describe the trend and the magnitude of a_3 reasonably well for all the particle species under study. Therefore, the simulations support Eq. (11), and verify another imprint of factorized actions. At $p_T > 1$ GeV/c, a_3 seems to have a smaller magnitude than $\tilde{a}_1 v_2$, which could be partially explained by the aforementioned anti-correlation between $\tilde{a}_1$ and v_2. The gradual breakdown of hydrodynamics towards higher p_T could also add to this discrepancy, since collective motions start to collapse.

While the search for the CME and the siCME continues as a subject of intensive investigation, we propose a feasible approach to assess the factorized-form approximation involving only the v_n coefficients. If directed flow and elliptic flow are approximately non-interdependent in Nature, the product of $(1+2\tilde{v}_1 \cos\Delta\varphi)$ and $(1 + 2\tilde{v}_2 \cos 2\Delta\varphi)$ yields a non-leading cross term, $4\tilde{v}_1\tilde{v}_2 \cos\Delta\phi \cos 2\Delta\phi = 2\tilde{v}_1\tilde{v}_2(\cos\Delta\phi + \cos 3\Delta\phi)$, similar to Eq. (2). Therefore, the v_1 observed with a linear Fourier expansion will be the true $\tilde{v}_1$ scaled by a factor of $(1 + \tilde{v}_2)$, and the observed v_3 will contain a rapidity-odd component of $\tilde{v}_1\tilde{v}_2$ on top of the existing rapidity-even $\tilde{v}_3$, if any. With respect to the reaction plane, $\tilde{v}_3$ is likely

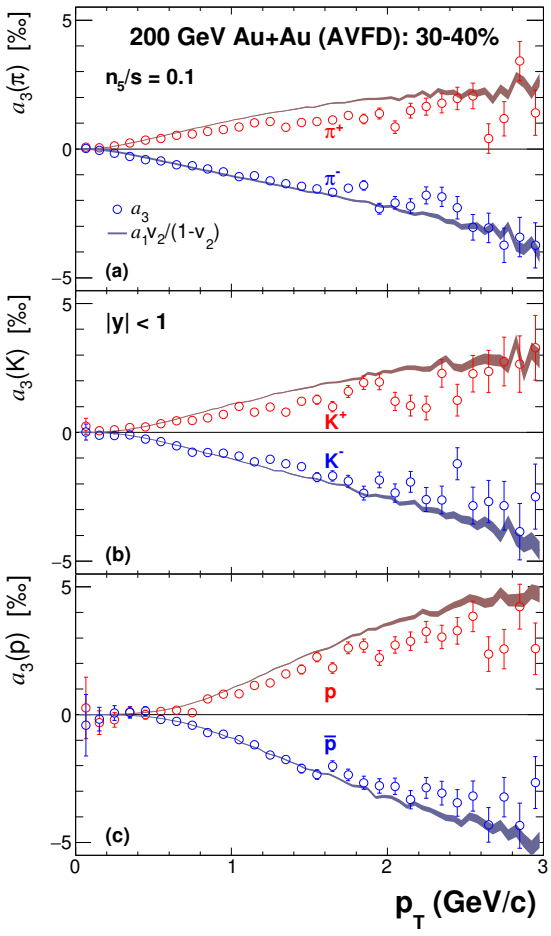


FIG. 3. EBE-AVFD simulations of a_3 as a function of p_T in 30–40% Au+Au collisions at 200 GeV for (a) π^+ and π^-, for (b) K^+ and K^-, and for (c) p and $\bar{p}$. In comparison, the values of $a_1 v_2/(1-v_2)$ are shown with shaded bands.

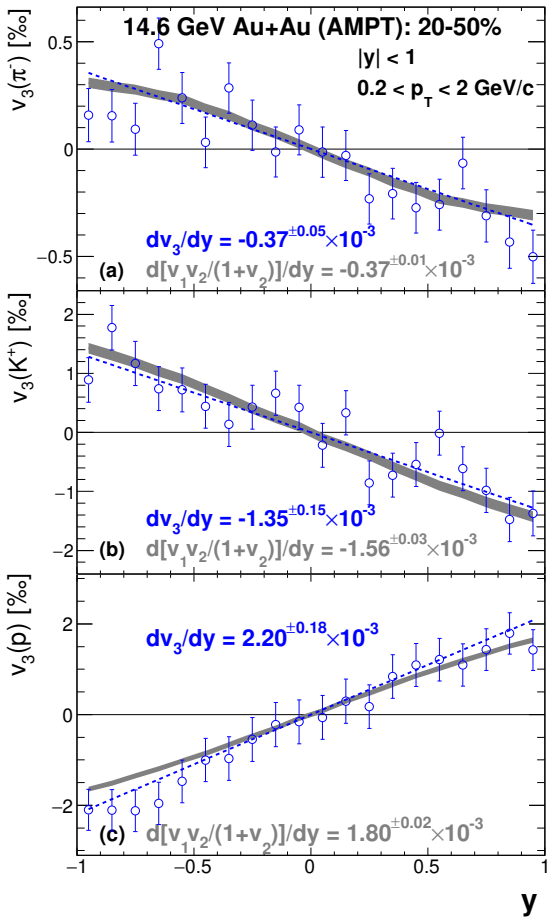


FIG. 4. AMPT simulations of v_3 vs y for (a) π^-, (b) K^+, and (c) p in 20–50% Au+Au collisions at 14.6 GeV. For comparison, the values of $v_1 v_2/(1+v_2)$ are shown with shaded bands. Linear fits are used to extract the slopes.

to be zero because the triangular anisotropy in the initial collision geometry is dominated by event-by-event fluctuations, and essentially decouples from the reaction plane [17]. Thus, the observation of a $v_3^{\rm odd}$ component establishes a signature of the factorized Fourier expansions. Along the same line of argument, the v_2 observed with the linear Fourier expansion will be the true $\tilde{v}_2$ scaled by $(1+\tilde{v}_4)$.

To test the aforementioned ideas, we exploit a multiphase transport (AMPT) model [18, 19], whose string melting version [19, 20] reproduces particle spectra and flow reasonably well at both RHIC and LHC energies [21]. We simulate Au+Au collisions at $\sqrt{s_{NN}} = 14.6$ GeV/c, where directed flow is prominent. Since the correlations between v_1 and v_2 and between v_2 and v_4 could be affected by pure mathematical relations similar to Eq. (12), we focus on $v_3^{\rm odd}$. Figure 4 presents AMPT calculations of v_3 vs y for (a) π^-, (b) K^+, and (c) p in the centrality range of 20–50%. We refrain from combining the results for particles and their antiparticles due to sizeable differences arising from transported-quark effects at this beam energy [22]. In each panel, we also include a shaded band to depict $v_1 v_2/(1+v_2)$ for comparison. For all studied particle species, the slope, dv_3/dy, is statistically significant and consistent with that of $v_1 v_2/(1+v_2)$, supporting the scenario of non-interdependent collective motions.

In summary, we stipulate that collective motions in high-energy heavy-ion collisions may be non-interdependent, and that the particle azimuthal distribution can take a factorized form that complements the widely-used long linear Fourier series. This scheme is more self-consistent, better captures the genuine strength of each collectivity mode, and makes new predictions based on non-leading cross terms. In the experimental extraction of Fourier coefficients, concerns of factorization or rather lack thereof have been raised from the viewpoint of nonflow [23–25] or decorrelation [26, 27], but none of them involves non-interdependent collective motions or their effects on the particle distribution. As a concrete example, we focus on the extra cross terms between the CME-induced $\tilde{a}_1$, the siCME-induced $\tilde{a}_3$, and elliptic flow v_2, and make two predictions. First,

the presence of a finite elliptic flow will scale $\tilde{a}_1$ by a factor of $(1 - v_2)$, and this effect is more important at higher p_T, where v_2 is larger. Since most CME-sensitive observables contain a_1^2, the corresponding reduction factor should be about $(1 - v_2)^2$. Second, as confirmed by the EBE-AVFD calculations, the observed a_3 receives a sizeable contribution from $\tilde{a}_1 v_2$, which complicates the interpretation of this siCME sensitive observable. Nevertheless, a finite a_3, if confirmed, constituents a strong evidence of the CME, whether it originates from $\tilde{a}_3$ or $\tilde{a}_1 v_2$ or both. We have also proposed a test to examine non-interdependent collective motions using the v_n coefficients, and the AMPT simulations corroborate the prediction of the rapidity-odd component of v_3. The universality of the assumption regarding factorized actions can be investigated through analyzing real data collected from RHIC and the LHC, which will enhance our understanding of the collective motions.

ACKNOWLEDGMENTS

The authors thank Shuzhe Shi and Jinfeng Liao for providing the EBE-AVFD code and for many fruitful discussions on the CME. We also thank Yufu Lin for generating the EBE-AVFD events. We thank Zi-Wei Lin and Guo-Liang Ma for providing the AMPT code. We are especially grateful to Zhongling Ji and Yicheng Feng for the fruitful discussions. Z. Xu, G. Wang and H. Huang are supported by the U.S. Department of Energy under Grant No. DE-FG02-88ER40424 and by the National Natural Science Foundation of China under Contract No.1835002. A.H. Tang is supported by the U.S. Department of Energy under Grants No. DE-AC02-98CH10886 and DE-FG02-89ER40531.

[1] P. Bozek and I. Wyskiel, Phys. Rev. C **81**, 054902 (2010).
[2] U. Heinz and R. Snellings, Ann. Rev. Nucl. Part. Sci. **63**, 123 (2013).
[3] D. E. Kharzeev, L. D. McLerran and H. J. Warringa, Nucl. Phys. A **803**, 227 (2008).
[4] D. Kharzeev, R. D. Pisarski, M. H. G. Tytgat, Phys. Rev. Lett. **81**, 512 (1998).
[5] V. Voronyuk, V. D. Toneev, W. Cassing, E. L. Bratkovskaya, V. P. Konchakovski, S. A. Voloshin, Phys. Rev. C **83**, 054911 (2011).
[6] M. Buzzegoli, D. E. Kharzeev, Y.-C. Liu, S. Shi, S. A. Voloshin, H.-U. Yee, Phys. Rev. C **106**, L051902 (2022).
[7] A. M. Poskanzer and S. A. Voloshin, Phys. Rev. C **58**, 1671 (1998).
[8] S. Shi, Y. Jiang, E. Lilleskov, J. Liao, Ann. Phys. **394**, 50 (2018).
[9] Y. Jiang, S. Shi, Y. Yin and J. Liao, Chin. Phys. C **42**, no. 1, 011001 (2018).
[10] S. Shi, H. Zhang, D. Hou and J. Liao, Phys. Rev. Lett. **125**, 242301 (2020).
[11] S. Choudhury et al, Chin. Phys. C **46** 014101 (2022).
[12] B.B. Back *et al.*, Phys. Rev. C **65**, 031901(R) (2002); K. Adcox *et al.*, Phys. Rev. Lett. **86**, 3500 (2001); I.G. Bearden *et al.*, Phys. Lett. B **523**, 227 (2001); J. Adams *et al.*, arXiv:nucl-ex/0311017.
[13] C. Shen, Z. Qiu, H. Song, J. Bernhard, S. Bass and U. Heinz, Comput. Phys. Commun. **199**, 61 (2016).
[14] V. Greco and C. Ko, Phys. Rev. C **70**, 024901 (2004).
[15] X. Dong, S. Esumi, P. Sorensen, N. Xu and Z. Xu, Phys. Lett. B **597**, 328 (2004).
[16] Z. Lin and C. Ko, Phys. Rev. Lett. **89**, 202302 (2002).
[17] B. Alver and G. Roland, Phys. Rev. C **81**, 054905 (2010); Erratum Phys. Rev. C **82**, 039903 (2010).
[18] B. Zhang, C.M. Ko, B.-A. Li and Z.-W. Lin, Phys. Rev. C **61**, 067901 (2000).
[19] Z.-W. Lin, C.M. Ko, B.-A. Li and B. Zhang, Phys. Rev. C **72**, 064901 (2005).
[20] Z.-W. Lin and C.M. Ko, Phys. Rev. C **65**, 034904 (2002).
[21] Z.-W. Lin, Phys. Rev. C **90**, 014904 (2014).
[22] L. Adamczyk *et al.* [STAR Collaboration], Phys. Rev. Lett. **120**, 62301 (2018).
[23] F. Gardim, F. Grassi, M. Luzum and J.-Y. Ollitrault, Phys. Rev. C **87** 031901 (R) (2013).
[24] S.H. Lim, Q. Hu, R. Belmont, K.K. Hill, J.L. Nagle, and D.V. Perepelitsa, Phys. Rev. C **100** 024908 (2019).
[25] D. Kikola, L.Yi, S. Esumi, F. Wang and W. Xie, Phys. Rev. C **86**, 014901 (2012).
[26] Piotr Bozek, Phys. Rev. C **98** 064906 (2018).
[27] L. Barbosa *et al.*, arXiv:2105.12792 (2021).